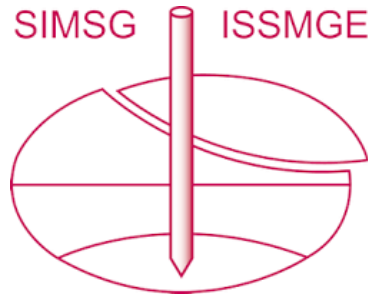


INTERNATIONAL SOCIETY FOR SOIL MECHANICS AND GEOTECHNICAL ENGINEERING



This paper was downloaded from the Online Library of the International Society for Soil Mechanics and Geotechnical Engineering (ISSMGE). The library is available here:

<https://www.issmge.org/publications/online-library>

This is an open-access database that archives thousands of papers published under the Auspices of the ISSMGE and maintained by the Innovation and Development Committee of ISSMGE.

The paper was published in the proceedings of the 10th European Conference on Numerical Methods in Geotechnical Engineering and was edited by Lidija Zdravkovic, Stavroula Kontoe, Aikaterini Tsiampousi and David Taborda. The conference was held from June 26th to June 28th 2023 at the Imperial College London, United Kingdom.

To see the complete list of papers in the proceedings visit the link below:

<https://issmge.org/files/NUMGE2023-Preface.pdf>

A Jacobi eigenvalue solver for material point models and one-dimensional consolidation simulations of a soil layer

C.D. Rodríguez^{1,2}, L. Canales-Brenlla¹, L.F. Prada-Sarmiento^{1,3}, T. Wichtmann¹

¹*Chair of Soil Mechanics, Foundation Engineering and Environmental Geotechnics,
Ruhr-Universität Bochum, Germany*

²*Chair of geotechnics, Bauhaus-Universität Weimar, Germany*

³*Department of Civil and Architectural Engineering, Aarhus University, Denmark*

ABSTRACT: The Material-Point Method (MPM) is used in this study to identify the eigenfrequencies and mode shapes of an elastic plane strain slice (column) that resembles a soil layer. The soil layer is also subjected to one-dimensional consolidation under a uniform vertical stress and modelled with MPM. The eigenvalue identification of the soil column is based on a generalised Jacobi method using Material-Point stiffness and mass matrices. To simulate the consolidation process, an explicit v - w formulation for fully saturated soils has been implemented into a Material-Point algorithm following existing approaches and making use of similar computational schemes. Simulations with different plane strain elements and different levels of spatial discretisation are performed to compare numerical results with analytical solutions. Finally, the algorithm for explicit time-integration is found to be numerically stable when adopting time-step sizes below reference critical values, e.g., values based on the Courant-Friedrichs-Lewy (CFL) stability condition, and on an analogy to a mass-spring oscillator that depends on the numerically obtained fundamental frequency of the model.

Keywords: MPM; consolidation; Jacobi method

1 INTRODUCTION

The MPM is a numerical technique developed initially by Sulsky et al. (1994, 1995) for the simulation of large deformation of solids, which shares theoretical and numerical aspects with the Finite Element Method (FEM). MPM simulations require the definition of a conventional finite element mesh and a set of material points representing the solid. Therefore, MPM has both a mesh- and particle-based nature rather than only the latter. As it was the case in the first formulations, which continue to be an approach followed in certain current developments, explicit time-integration schemes have been adopted. Nonetheless, recent progress has focused on establishing a stable numerical framework for implicit calculations, e.g. see Zheng et al. (2022). Moreover, the MPM is suitable for the simulation of boundary-value problems in geotechnics involving both large and small deformations. For this reason, it can be seen as a general numerical tool for a variety of applications in geotechnics, ranging from geohazards to some classical boundary-value problems.

This paper presents the suitability of the MPM to perform eigenvalue identification and studies its usefulness in simulating the consolidation process without the need to adopt numerical stabilisation techniques. This paper solves a benchmark problem for one-dimensional consolidation using an explicit MPM algorithm under plane-strain conditions. Simulations with low- and

high-order quadrilateral elements and low-order element models with different mesh element sizes are performed to assess the element type and spatial discretisation effect, respectively. For this purpose, the critical time-step size selection is made considering limit criteria to ensure numerical stability, e.g. CFL stability condition. Additionally, the time-step size of the models with a background grid of 10 elements are computed based on their numerically obtained fundamental frequencies. An eigenvalue solver was employed by assembling stiffness and consistent mass matrices that are in accordance with implicit MPM schemes. From the mathematical point of view this paper presents an alternative to effectively compute eigenfrequencies and mode shapes of MPM models using existing and well-established mathematical transformation tools of system matrices.

Notation: In this paper, matrices and second-order tensors are denoted with bold capital letters (e.g. \mathbf{M} , \mathbf{K} , $\boldsymbol{\sigma}$, $\boldsymbol{\Lambda}$, $\boldsymbol{\Phi}$), vectors and tensors of rank one are represented with lowercase bold letters (e.g. \mathbf{u} , $\ddot{\mathbf{u}}$, $\boldsymbol{\varphi}$), and scalars and other variables are written in lowercase or capital letters without bold (e.g. ϱ , α_{ij} , λ , V , L).

1.1 The Jacobi method as eigenvalue solver

There are several methods to solve eigenvalue problems of numerical models, namely vector iteration, transformation, polynomial iteration and Sturm sequence, Lanczos iteration and subspace iteration methods (see Bathe (2014) and Noble and Daniel (1977)). One well-known, effective and straightforward procedure is the generalised Jacobi method (Hughes, 1987), which satisfies a transformation requirement. The technique was first proposed by Jacobi (1846) and meets the conditions of a transformation method for eigenvalue problems, reducing the global matrices to diagonal form numerically.

In particular, the Jacobi method, in combination with FEM, has been employed on soil structure interaction problems (Zangeneh et al., 2021); (Béliveau, 1977) and the solution of Biot's consolidation equations (Phoon et al., 2002).

1.2 MPM Hydro-mechanical formulations

After the original MPM one-phase formulation (Sulsky et al., 1994, 1995), several approaches that account for hydro-mechanical interaction have been proposed. The two main spatial discretisation strategies within the MPM framework vary from single- to double-layer schemes. The soil can be represented by solid (grains), liquid and gas phases to describe porous media behaviour in a more generalised condition (i.e., partially saturated). Saturated conditions can be considered as a sub-case when the gas phase is not present. The single-layer approach offers a straightforward formulation and implementation among the main strategies. For example, the approach has been applied to simulate dam failure (Zabala and Alonso, 2011), wave attack on sea dikes (Jassim et al., 2013), rainfall effects on an embankment slope (Yerro et al., 2015) or piezocene penetration tests (Ceccato et al., 2016). Alternatively, double-point schemes involve the implementation of a distinct set of material points to describe each phase respectively, e.g. set of solid material points and liquid material points, allowing for the simulation of seepage effects and induced levee failure (Abe et al., 2014; Bandara and Soga, 2015).

Additionally, recent coupling strategies include MPM -FEM coupling (Pan et al., 2021) for the simulation of wave-induced phenomena, MPM-SPH coupling (Nakamichi et al., 2021) for fully-water saturated conditions or MPM-FVM coupling (Baumgarten et al., 2021) for applications involving gas seepage and erosion caused by air flows.

In this paper, the existing two-phase single-layer approach has been implemented in Python and used to simulate one-dimensional consolidation processes.

2 GOVERNING EQUATIONS

2.1 The generalized Jacobi Method for a MP model

In the generalised Jacobi method, local stiffness and mass matrices are first calculated at grid cells of a material point idealised system, following numerical approximation to the integrals over the domain Ω . In particular, material-point approximation has been used as shown in Equations (1).

$$\mathbf{K} = \int_{\Omega} \mathbf{B}^T \mathbf{D} \mathbf{B} \, d\Omega \approx \sum_{p=1}^{mp} \mathbf{B}_p^T \mathbf{D}_p \mathbf{B}_p \frac{m_p}{\rho_p} \quad (1)$$

$$\mathbf{M} = \int_{\Omega} \mathbf{H}^T \rho \mathbf{H} \, d\Omega \approx \sum_{p=1}^{mp} m_p \mathbf{H}_p^T \mathbf{H}_p$$

where \mathbf{K} and \mathbf{M} are the linear stiffness matrix and the consistent mass matrix of an MP numerical model respectively. This approach is adopted from implicit formulations of the MPM like those proposed by Wang et al. (2016) and Guilkey and Weiss (2003).

The algorithm: the procedure aims at a systematic reduction of the system matrices over sweeps by means of a rotation matrix \mathbf{P} in the following manner:

$$\mathbf{A}^{k+1} = \mathbf{P}^T \mathbf{A}^k \mathbf{P}^k \quad (2)$$

where \mathbf{A} is a global matrix of the discrete system and k is the sweep counter. The rotation matrices \mathbf{P} consist of ones on their diagonal and elements γ_{ij} and α_{ij} below and above its diagonal respectively. The values γ_{ij} and α_{ij} are obtained from the solution of the system of equations (3).

$$\alpha_{ij} K_{ii}^k + (1 + \alpha_{ij} \gamma_{ij}) K_{ij}^k + \gamma_{ij} K_{jj}^k = 0 \quad (3)$$

$$\alpha_{ij} M_{ii}^k + (1 + \alpha_{ij} \gamma_{ij}) M_{ij}^k + \gamma_{ij} M_{jj}^k = 0$$

Convergence is attained when the off-diagonal elements of the stiffness and mass matrices have been zeroed or are very close to zero. In this paper the following criteria have been used:

$$\sqrt{\frac{(A_{ij}^{k+1})^2}{|A_{ii}^{k+1} A_{jj}^{k+1}|}} \leq \xi \quad \text{and} \quad \frac{|A_{ii}^{k+1} - A_{jj}^k|}{A_{ij}^{k+1}} \leq \xi \quad (4)$$

$$\mathbf{\Lambda} = \text{diag} \left(\frac{K_{ii}^{l+1}}{M_{ii}^{l+1}} \right) \quad (5a)$$

$$\mathbf{\Phi} = \mathbf{P}^1 \mathbf{P}^2 \dots \mathbf{P}^l \left((M_{ii}^{l+1})^{-\frac{1}{2}} \right) \quad (5b)$$

where ζ is the tolerance used for zeroing the off-diagonal elements of \mathbf{K} and \mathbf{M} . This criteria slightly differs from Bathe (2014); the absolute value of the product $A_{ii}^{k+1}A_{jj}^{k+1}$ is added to the denominator of the first ratio in Equation (4) to avoid the comparison of ζ with complex quantities. Once the criteria are met, the eigenvalues and eigenvectors of the MP system can be obtained as shown in Equations (5) where l is the penultimate sweep performed before meeting the convergence criteria.

2.2 v-w coupled formulation for soils

The v-w formulation, equivalent to the u-U formulation within the FEM context (Zienkiewicz et al., 1999), has been implemented following Yerro and Rohe (2019) and Jassim et al. (2013). Hence, only a computational cycle of the existing approach is presented here. In this approach, the primary variables are the acceleration vectors of the solid $\ddot{\mathbf{u}}_s$ and liquid $\ddot{\mathbf{u}}_l$ phases. The subscripts s and l denote the solid and liquid phases, respectively. The time-integration scheme hereby adopted is the explicit Euler forward method (Equations (6))

$$\dot{\mathbf{u}}^{k+1} = \dot{\mathbf{u}}^k + \Delta t \ddot{\mathbf{u}}^k \quad (6)$$

$$\mathbf{u}^{k+1} = \mathbf{u}^k + \Delta t \dot{\mathbf{u}}^{k+1}$$

A critical time-step Δt_{crit} to ensure numerical stability has been defined as the minimum time step between four criteria (see Table 1). The $\Delta t_{\text{crit,CFL}}$ corresponds to the standard CFL stability condition (Bathe, 2014), $\Delta t_{\text{crit},1}$ to undrained conditions (Jassim et al., 2013), $\Delta t_{\text{crit},2}$ to diffusion problems (Jassim et al.; 2013) and $\Delta t_{\text{crit},3}$ to an analogy of a mass-spring oscillator. L_{min} is the smallest length of a finite element, and c is the speed of sound of a compression wave.

Table 1. Summary of critical time-step criterion considered.

Description	Criterion (c_i)
$\Delta t_{\text{crit,CFL}} = L_{\text{min}}/c$	$\sqrt{E_c/\rho}$
$\Delta t_{\text{crit},1} = L_{\text{min}}/c_1$	$\sqrt{(E_c + (K_l/n_l))/\rho_m}$
$\Delta t_{\text{crit},2} = L_{\text{min}}^2/(2c_2)$	$\frac{k}{\gamma_w(1/E_c + n_l/K_l)}$
$\Delta t_{\text{crit},3} = L_{\text{min}}/c_3$	$2f_1 \cdot L \cdot \pi$

$$\dot{n}_l = n_s \text{div}(\dot{\mathbf{u}}_s) \quad (7)$$

$$\dot{\epsilon}_{\text{vol}} = \frac{1}{n_l} [n_s \text{div}(\dot{\mathbf{u}}_s) + n_l \text{div}(\dot{\mathbf{u}}_l)] \quad (8)$$

$$\dot{p}_l = K_l \dot{\epsilon}_{\text{vol}} \quad (9)$$

Governing equations involve the conservation of mass and momentum. Although the mass of the solid phase m_s is constant, the total mass in each material point can vary depending on the in- or out-flow of the liquid mass m_l . The mass balance of the solid phase can be expressed as an expression of porosity rate (7) by assuming an incompressible solid, a weakly compressible liquid and ignoring spatial variations in density and porosity. Here, the volumetric concentration of the liquid phase n_l will be identical to the porosity of the soil n in a saturated condition and $n_l + n_s = 1$. Likewise, the mass balance equation of the mixture is simplified to Equation (8), describing the volumetric strain rate, and is also used to define the pore pressure rate as written in Equation (9) (Jassim et al., 2013).

$$n_s \rho_s \ddot{\mathbf{u}}_s + n_l \rho_l \ddot{\mathbf{u}}_l = \text{div}(\boldsymbol{\sigma}) + \rho_m \mathbf{b} \quad (10)$$

$$\rho_l \ddot{\mathbf{u}}_l = \nabla p_l - \mathbf{f}_l^d + \rho_m \mathbf{b} \quad (11)$$

$$\mathbf{f}_l^d = \frac{n_l \mu_l}{\kappa_l} (\dot{\mathbf{u}}_l - \dot{\mathbf{u}}_s) \quad \text{with } \kappa_l = k_l \frac{\mu_l}{\rho_l g} \quad (12)$$

The momentum balance of the mixture and momentum balance of the liquid phase are written in Equations (10,11), respectively. The drag force \mathbf{f}_l^d is defined according to laminar and stationary flow conditions in the slow velocity regime, i.e., Darcy law validity (Equation (12)) where p_l is the liquid pressure, μ_l represents the dynamic viscosity of the liquid, κ_l is the liquid's intrinsic permeability and k_l refers to Darcy's permeability. A weak formulation and discretisation of the momentum balance equations results in Equation (13) for the momentum balance of the mixture and Equation (14) for the momentum balance of the liquid phase Yerro and Rohe (2019).

$$\mathbf{M}_s \ddot{\mathbf{u}}_s + \mathbf{M}_l \ddot{\mathbf{u}}_l = \mathbf{f}_m^{\text{ext}} - \mathbf{f}_m^{\text{int}} \quad (13)$$

$$\tilde{\mathbf{M}}_l \ddot{\mathbf{u}}_l = \mathbf{f}_m^{\text{ext}} - \mathbf{f}_m^{\text{int}} - \mathbf{Q}_l (\dot{\mathbf{u}}_l - \dot{\mathbf{u}}_s) \quad (14)$$

$$\boldsymbol{\sigma} = \boldsymbol{\sigma}' + \mathbf{m} p_l \quad (15)$$

where \mathbf{M} term denotes a lumped mass matrix and \mathbf{Q}_l is the drag force matrix. $\ddot{\mathbf{u}}$, $\dot{\mathbf{u}}$ and \mathbf{f} denote acceleration, velocity and force vectors at a nodal level, respectively. Effective stresses are computed based on total stresses $\boldsymbol{\sigma}$ and pore pressures p_l with $\mathbf{m}=(111000)^T$.

3 AN ELASTIC SOIL LAYER

A 1-meter-high linear-elastic soil layer under plain strain conditions is considered here by modelling a slice (column) of soil 0.1 m; different levels of mesh discretisation are considered, as shown in Figure 1.

Only vertical displacement is allowed along the lateral boundaries and the bottom boundary is fixed in both directions, thus, imposing single-drainage conditions. A surface load of $q = 10$ kPa is applied at the ground surface and kept constant. The soil and flow parameters are summarised in Table 2. Moreover, the Bulk modulus of the water has been chosen below physical values of fully saturated conditions to decrease the computational time of the consolidation simulations although only fully saturated problems are dealt with here.

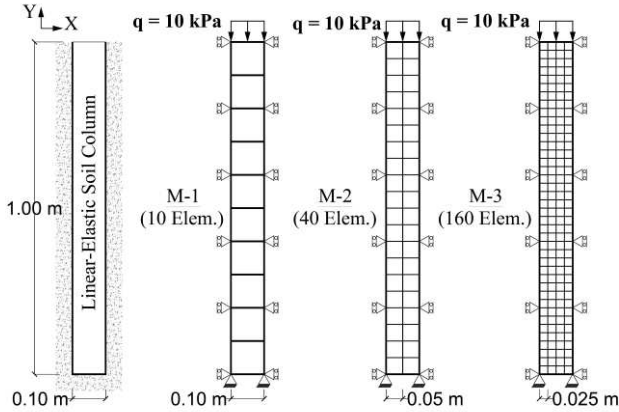


Figure 1. Numerical models

Table 2. Soil and flow parameters

Parameter	Symbol	Unit	Value
Solid Density	ρ_s	kg/m ³	2,700
Liquid Density	ρ_l	kg/m ³	1,000
Young's Modulus	E	kPa	10,000
Liquid Bulk Modulus	K_l	kPa	120,000
Porosity	n	–	0.3
Liquid Dynamic Viscosity	μ_l	kg/ms	1×10^{-3}
Hydraulic Conductivity	k	m/s	2.5×10^{-4}

4 EIGENVALUE IDENTIFICATION OF THE 2D SOIL SLICE

Eigenvalue identification of three different numerical models of the soil slice/column consisting of quadrilateral plane strain elements of a different order were performed using the generalised Jacobi Method. The elements used were bi-linear 4-noded, bi-quadratic 8-noded and 9-noded. The model with 4-noded elements contains four material points per element, while the models with 8-noded and 9-noded (Lagrangian) elements have nine. A tolerance of $\xi = 10-15$ has been chosen. Convergence was found after 7 and 9 sweeps on the models with 4 and 9 material-points per element, respectively.

Figure 2 shows the first 5 mode shapes of the 9-noded soil column model. Additionally, a finite element model

was generated in Abaqus using bi-quadratic fully interpolated plane strain elements (CPE8) and a matching mesh to that of the material point models. A frequency analysis to determine the eigenvalues and eigenvectors using the Lanczos iteration method implemented in Abaqus was performed (Parlett and Scott, 1979; Parlett, 1998; Grimes et al., 1994). A comparison of eigenvalues between models is shown in Table 3; the maximum difference found between the eigenfrequencies of the finite element model and its equivalent 8-noded material point model is below 1%.

Table 3. First 5 natural frequencies in Hz - comparison between MP models and a finite element model

Mode	4-noded	8-noded	9-noded	Abaqus CPE8
1	16.92	16.89	16.89	16.89
2	51.27	50.62	50.62	50.68
3	87.24	84.20	84.20	84.49
4	126.03	117.62	117.62	118.37
5	168.95	150.94	150.94	152.42

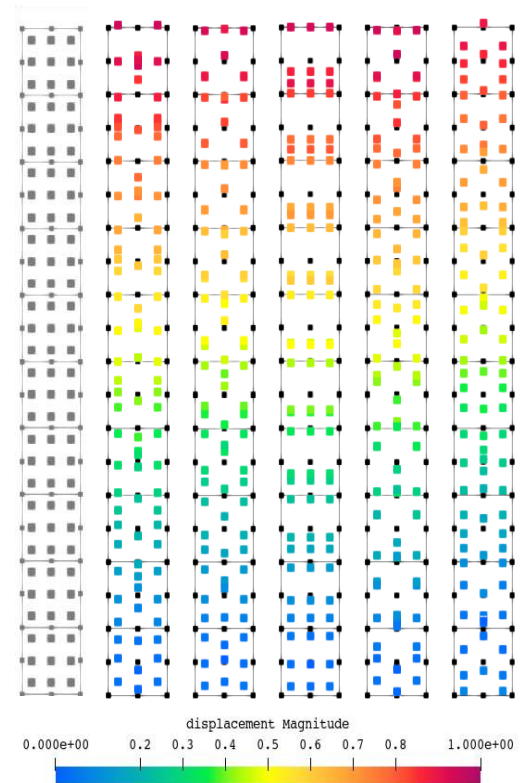


Figure 2. Mode shapes with 9-noded elements

The smallest vertical compression wave velocity c of the soil layer is estimated based on the fundamental frequency of the MP models f_1 as a single spring-mass oscillator (see also Table 1). With a frequency of 16.89 Hz the vertical compression wave velocity is $c_3 = 106.10$ m/s.

5 ONE DIMENSIONAL CONSOLIDATION

The appropriate time-step was selected based on the criteria of Table 1. As a result, $\Delta t_{crit,1}$ was found to govern in all cases. The critical time step sizes for the models M1, M2 and M3 (see Figure 1) are 2.31×10^{-4} s, 1.16×10^{-4} s and 5.78×10^{-5} s, respectively. The adopted critical times are 10^{-4} s for M1 and M2, and 5×10^{-5} s for M3.

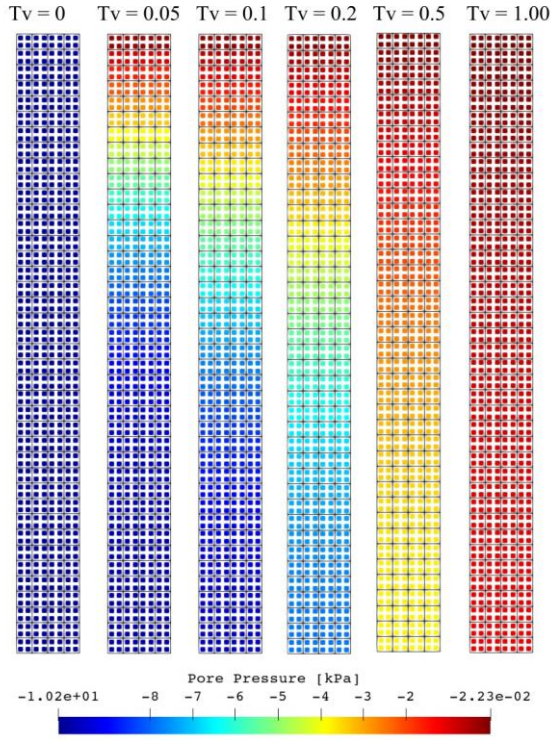


Figure 3. M-3 with 640 MPs - Pore pressure field

Table 4. Normalised. pore pressure and percent error comparison between different element orders

Tv	4-noded	8-noded	9-noded
0.02	0.996 (0.50 %)	0.961 (2.92 %)	0.974 (1.66 %)
0.5	0.289 (6.17 %)	0.274 (1.85 %)	0.273 (1.35 %)
1	0.086 (8.68 %)	0.082 (4.64 %)	0.082 (4.90 %)

Table 5. Normalised pore pressure and error - Spatial discretisation

Tv	M-1	M-2	M-3
0.02	0.996 (0.50 %)	0.991 (0.10 %)	0.990 (0.10 %)
0.5	0.289 (6.17 %)	0.280 (4.59 %)	0.275 (3.70 %)
1	0.086 (8.68 %)	0.084 (7.33 %)	0.082 (6.48 %)

Fields of pore pressure are shown in Figure 3. Furthermore, simulations of model M-1 with different plane strain elements (see Figure 4) show that results obtained with high-order elements are closer to the analytical solution. The numerical results are compared to the analytical solution of one-dimensional consolidation of Terzaghi including his definition of

dimensionless time factor T_v . The error of the solutions with different models is shown in Table 4. Finally, it can be concluded from Figure 5 and Table 5 that results of numerical simulations with a finer discretisation level, both in terms of the mesh element size and the total number of material points, lead to more accurate results.

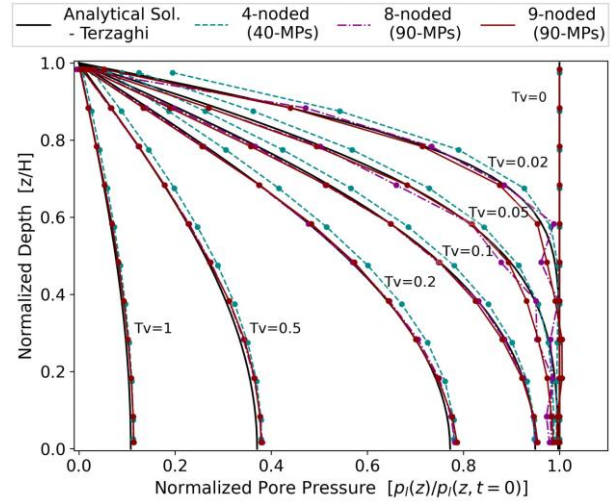


Figure 4. M-1 with different element orders

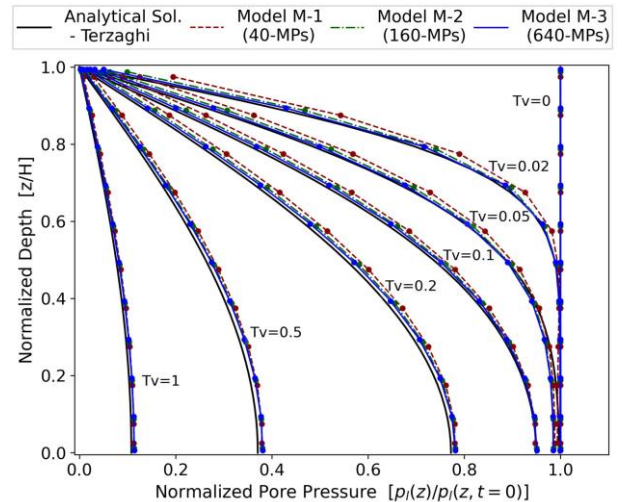


Figure 5. M-1, M-2, and M-3 - Spatial discretization effect

6 CONCLUSIONS

The generalised Jacobi method was effectively applied on material point models to perform eigenfrequency analysis. The algorithm presented in this paper proved efficient by using a tolerance value one thousand times smaller than that suggested by Bathe (2014). The natural frequencies matched those obtained with a finite element approach using fully integrated finite elements. The differences in the natural frequencies between the 8-noded model and the CPE8 model of Abaqus can be attributed to the different solvers behind the solution of the generalised eigenvalue problem and to the fact that material points do not exactly match Gauss point locations. Additionally, the fundamental frequencies of the

material point models were used to estimate the smallest numerically-obtained compression wave velocity of the soil layer; subsequently, employing this velocity as an additional criterion to estimate critical time steps. However, the CFL condition governed in all cases. In particular, the numerical simulations of the consolidation process showed an overall close agreement with the analytical solution. They achieved numerical stability when an appropriate time-step size was adopted, even without resorting to stabilisation techniques. In this context, the initial pore pressure oscillation present in particular simulations has been attributed in the literature to wave reflection effects, e.g. Jassim et al. (2013). These initial oscillations are "naturally" suppressed by the stabilising factor inherently present in the momentum balance equation of the liquid phase by the dragging force term. If this effect was to be directly mitigated, the inclusion of energy dissipation in the form of bulk viscosity, viscous boundaries or artificial damping can be considered. Finally, it has been shown that the employment of high-order elements resulted in an altogether closer agreement with the analytical solution and that a finer level of spatial discretisation resulted in improved numerical accuracy.

7 REFERENCES

- Abe, K., Soga, K. and Bandara, S. (2014), 'Material Point Method for Coupled Hydro-mechanical Problems', *Journal of Geotechnical and Geoenvironmental Engineering* 140(3), 04013033.
- Bandara, S. and Soga, K. (2015), 'Coupling of soil deformation and pore fluid flow using material point method', *Computers and Geotechnics* 63, 199–214.
- Bathe, K.-J. (2014), *Finite element procedures*, 2nd ed edn, Prentice-Hall. OCLC: ocn930843107.
- Baumgarten, A. S., Couchman, B. L. and Kamrin, K. (2021), 'A coupled finite volume and material point method for two-phase simulation of liquid–sediment and gas–sediment flows', *Computer Methods in Applied Mechanics and Engineering* 384, 113940.
- Béliveau, J. G. (1977), 'Parameter estimation from nonnormal modes of soil-structure interaction', *Journal of Optimization Theory and Applications* 23(1), 41–51.
- Ceccato, F., Beuth, L. and Simonini, P. (2016), 'Analysis of Piezocone Penetration under Different Drainage Conditions with the Two-Phase Material Point Method', *Journal of Geotechnical and Geoenvironmental Engineering* 142(12), 04016066.
- Fern, J., Rohe, A., Soga, K. and Alonso, E. (2019), *The Material Point Method for Geotechnical Engineering: A Practical Guide*, CRC Press, Boca Raton : CRC Press, Taylor & Francis Group.
- Grimes, R. G., Lewis, J. G. and Simon, H. D. (1994), 'A shifted block lanczos algorithm for solving sparse symmetric generalised eigenproblems', *SIAM Journal on Matrix Analysis and Applications* 15(1), 228–272.
- Guilkey, J. E. and Weiss, J. A. (2003), 'Implicit time integration for the material point method: Quantitative and algorithmic comparisons with the finite element method', *International Journal for Numerical Methods in Engineering* 57(9), 1323–1338.
- Hughes, T. J. R. (1987), *The finite element method: linear static and dynamic finite element analysis*, Prentice-Hall.
- Jacobi, C. (1846), 'Über ein leichtes verfahren die in der theorie der säcularstörungen vorkommenden gleichungen numerisch aufzulösen', *Journal für die reine und angewandte Mathematik (Crelles Journal)* 1846(30), 51–94.
- Jassim, I., Stolle, D. and Vermeer, P. (2013), 'Two-phase dynamic analysis by material point method', *International Journal for Numerical and Analytical Methods in Geomechanics* 37(15), 2502–2522.
- Nakamichi, Y., Sugie, S. and Takeyama, T. (2021), A Coupled MPM–SPH Numerical Simulation for Fully Saturated Soil, pp. 794–801.
- Noble, B. and Daniel, J. W. (1977), *Applied linear algebra*, 2d ed edn, Prentice Hall.
- Pan, S., Yamaguchi, Y., Suppasri, A., Moriguchi, S. and Terada, K. (2021), 'MPM–FEM hybrid method for granular mass–water interaction problems', *Computational Mechanics* 68(1), 155–173.
- Parlett, B. N. (1998), *The Symmetric Eigenvalue Problem*, Society for Industrial and Applied Mathematics.
- Parlett, B. N. and Scott, D. S. (1979), 'The lanczos algorithm with selective orthogonalisation', *Mathematics of Computation* 33(145), 217–238.
- Phoon, K. K., Toh, K. C., Chan, S. H. and Lee, F. H. (2002), 'An efficient diagonal preconditioner for finite element solution of biot's consolidation equations', *International Journal for Numerical Methods in Engineering* 55(4), 377–400.
- Sulsky, D., Chen, Z. and Schreyer, H. (1994), 'A particle method for history-dependent materials', *Computer Methods in Applied Mechanics and Engineering* 118(1-2), 179–196.
- Sulsky, D., Zhou, S.-J. and Schreyer, H. (1995), 'Application of a particle-in-cell method to solid mechanics', *Computer Physics Communications* 87(1-2), 236–252.
- Terzaghi, K., Peck, R. B. and Mesri, G. (1996), *Soil Mechanics in Engineering Practice*, John Wiley & Sons, Inc.
- Wang, B., Vardon, P. J., Hicks, M. A. and Chen, Z. (2016), 'Development of an implicit material point method for geotechnical applications', *Computers and Geotechnics* 71, 159–167.
- Yerro, A., Alonso, E. and Pinyol, N. (2015), 'The material point method for unsaturated soils', *Géotechnique* 65(3), 201–217.
- Zabala, F. and Alonso, E. (2011), 'Progressive failure of Aznalcóllar dam using the material point method', *Géotechnique* 61(9), 795–808.
- Zangeneh, A., François, S., Lombaert, G. and Pacoste, C. (2021), 'Modal analysis of coupled soil-structure systems', *Soil Dynamics and Earthquake Engineering* 144, 106645.
- Zheng, X., Pisanò, F., Vardon, P. J. and Hicks, M. A. (2022), 'Fully implicit, stabilised MPM simulation of large-deformation problems in two-phase elastoplastic geomaterials', *Computers and Geotechnics* 147, 104771.
- Zienkiewicz, O., Chan, A., Pastor, M., Schrefler, B. and Shiomi, T. (1999), *Computational Geomechanics with Special Reference to Earthquake Engineering*, John Wiley & Sons.